ICRC 2001

Nonthermal X-ray emission from young supernova remnants

E. van der Swaluw[1] **and Bram Achterberg**[2]

[1]Dublin Institute for Advanced Studies, 5 Merrion Square, Dublin 2, Republic of Ireland
[2]Astronomical Institute, Utrecht University, P.O. Box 80000, 3508 TA Utrecht, The Netherlands

Abstract. The Galactic (nucleonic) cosmic-ray spectrum up to the knee ($E \sim 10^{15}$ eV) is believed to originate from acceleration processes occurring at supernova remnant shocks. This idea is confirmed by theoretical predictions, which give a similar estimate for the maximum particle energy, which can be reached at these shocks.

Electrons with energies $E \sim 10^{14}$ eV radiate X-ray photons in the $\sim 10 - 100$ μG magnetic fields present in many young supernova remnants. These electrons (near the knee), give rise to a nonthermal X-ray component in the spectrum of young supernova remnants. Recent observations of SN1006 and G347.3-0.5 show these nonthermal X-rays.

We have combined hydrodynamical calculations of the evolution of a young remnant with an algorithm which simultaneously calculates the associated particle acceleration, in the test-particle approximation.

We present the resulting synchrotron maps, at different X-ray frequencies, and photon spectra of the synchrotron radiation. Our method allows for calculating photon and electron spectra at different regions within the remnant.

1 Introduction

The origin of the cosmic-ray spectrum up to the knee ($E \sim 10^{15}$ eV) is attributed to the acceleration processes which occur at the shocks around supernova remnants (SNRs). The theory of diffusive shock acceleration (for a recent review of DSA see e.g. Malkov & Drury, 2001) predicts a power-law distribution in energy, $\phi(E) \propto E^2 f(E) \propto E^{-q}$, with $q = 2.0$, when the particles are accelerated by a strong shock (with compression ratio $r = 4.0$). This seems to contradict the observed energy spectrum of cosmic rays at earth:

$$\phi(E) \propto E^2 f(E) \propto E^{-2.7}. \tag{1}$$

However, this observed spectrum includes the effect of the propagation of the cosmic rays through the interstellar medium

Correspondence to: E. van der Swaluw (swaluw@cp.dias.ie)

(ISM), which leads to an increase in the slope q by a factor of $\sim 0.5 - 0.6$. A direct fingerprint of the slope of the power-law q can be obtained by radio observations of SNRs. The observed spectral index of the synchrotron emission from these systems, $\alpha \simeq 0.5 - 0.6$ is directly connected with the slope of the energy distribution q of the accelerated partricles by $q = 2\alpha + 1 \simeq 2.0 - 2.2$. This is close to the value one expects for the energy distribution of accelerated particles at a strong shock. There is no effect on the slope q due to the propagation of the electrons, as is the case for the nucleonic cosmic ray spectrum, because the observed synchrotron radiation is emitted by the electrons in the accelerator itself.

Using standard synchrotron radiation theory (see e.g. Rybicky & Lightmann, 1979), one can show that electrons radiating in a $\sim 10 - 100$ μG magnetic field, emit at radio frequencies when their energy is of order $\sim 10^{12}$ eV, whereas electrons radiating at X-ray frequencies have a typical energy of $\sim 10^{14}$ eV. This last value is close to the knee of the cosmic ray spectrum. Therefore the recent discoveries of supernova remnants with a nonthermal X-ray component (Koyama et al., 1995; Allen, Gotthelf & Petre, 1999; Slane et al., 2001), seems like another confirmation of the supernova-origin theory of cosmic rays.

In this paper we present a method which calculates the morphology and the spectrum of synchrotron X-rays from young supernova remnants. We use a hydrodynamics code to calculate the evolution of a SNR in a uniform interstellar medium. Simultaneously we calculate the acceleration of electrons injected at the shock bounding the SNR, using a separate algorithm which includes the effect of synchrotron and adiabatic losses. The simulations are performed using the test-particle approximation, which neglects the back reaction of the particles on the flow.

This paper is organised as follows. In section 2 we describe the evolution of a young SNR and the associated particle acceleration. In section 3 we present results of our method. Section 4 is a summary and prospects some future applications of our method.

2 Particle acceleration at SNR shocks

2.1 The evolution of a young SNR

A supernova explosion results in an expanding supernova remnant, which can roughly be divided into four stages (woltjer, 1972): the free expansion stage, the Sedov-Taylor stage, the pressure-driven snowplow stage and the momentum conserving stage. In the model presented here we will only focus on the first two stages. McKee & Truelove (1995) describe these two stages by giving analytical approximations for the trajectories of both the forward shock and the reverse shock of a SNR. The transition between these two stages takes place when the forward shock of the SNR has swept-up ~ 1.61 times the ejected mass of the progenitor star. This occurs at an age:

$$t_{ST} = 209 E_{51}^{-1/2} \left(\frac{M_{ej}}{M_\odot} \right)^{5/6} n_0^{-1/3} \ \text{yr}, \qquad (2)$$

where $n_0 = \rho_0 / \mu_m$ is the number density (in cm^{-3}) of the ISM, assuming a mean atomic mass $\mu_m = 2.34 \times 10^{-24}$ g. M_{ej} is the ejected mass of the progenitor star, and E_{51} is the mechanical explosion energy in units of 10^{51} erg. Below we will argue that particles are accelerated most efficiently at times $t \ll t_{ST}$.

2.2 Particle acceleration

A blastwave of a SNR is an efficient accelerator due to the efficient scattering of relativistic particles which confines these particles near the shock. Therefore particles can cross the shock many times before being advected downstream. Each time a particle crosses a shock from downstream $\rightarrow$ upstream $\rightarrow$ downstream it will gain energy due to the difference in velocity across the shock. The resulting spatial diffusion can be described by using the Bohm approximation. In this approximation, the scattering mean free path l equals the gyro radius $r_g \propto E/ZeB$ of a relativistic particle (energy $E = pc$), corresponding with a diffusion coefficient:

$$\kappa_B \equiv \frac{1}{3} c r_g = \frac{cE}{3ZeB}, \qquad (3)$$

here Ze is the particle charge and B is the magnetic field strength. This diffusion coefficient determines the acceleration rate using standard DSA where we only consider protons and electrons ($Z = 1$):

$$\left(\frac{dE}{dt} \right)_{dsa} = \frac{3}{\xi} \frac{eBV_s^2}{c}, \qquad (4)$$

here V_s is the shock velocity. The parameter ξ takes the value $\xi = 20$ for a parallel shock where the magnetic field is along the shock normal, and $\xi = 8$ for a perpendicular shock where the field is in the plane of the shock.

If the accelerated particles are electrons, they suffer radiative losses due to the presence of the magnetic field. These synchrotron losses equals (e.g. Rybicky & Lightman, 1979):

$$\left(\frac{dE}{dt} \right)_{sy} = -\frac{\sigma_T B^2 E^2}{6\pi m_e^2 c^3}, \qquad (5)$$

where $\sigma_T = 6.65 \times 10^{-25} \ cm^2$ is the Thomson cross section and m_e is the mass of an electron.

2.3 Maximum energies

If synchrotron losses can be neglected, as is the case for protons, using equation (4), one can show that the maximum energy equals:

$$E_{max} \approx 200 E_{51} \left(\frac{\xi}{10} \right)^{-1} \left(\frac{M_{ej}}{1 M_\odot} \right)^{-1/6} \times$$
$$\left(\frac{B}{10 \ \mu G} \right) n_0^{-1/3} \ \text{TeV} . \qquad (6)$$

Particles injected at the shock of the SNR at a time $t \ll t_{ST}$ will reach an energy E_{max} at $t \sim t_{ST}$. In the Sedov-Taylor stage the acceleration rate decays as $(dE/dt)_{dsa} \propto V_s^2 \propto R_{snr}^{-3}$. The acceleration process in the Sedov-Taylor stage can roughly increase the energy by a factor of 3. Therefore the acceleration process is most efficient at times $t \ll t_{ST}$.

If synchrotron losses can not be neglected as is the case for electrons, the combination of equation (4) and (5) shows that the maximum energy equals:

$$E_{sy} \approx 350 E_{51}^{1/2} \left(\frac{\xi}{10} \right)^{-1/2} \left(\frac{V_s}{V_{ST}} \right) \times$$
$$\left(\frac{M_{ej}}{M_\odot} \right)^{-1/2} \left(\frac{B}{10 \ \mu G} \right)^{-1/2} \ \text{TeV} . \qquad (7)$$

here V_{ST} is a typical velocity for a young SNR as defined by McKee & Truelove (1995):

$$V_{ST} = 10,400 E_{51}^{1/2} \left(\frac{M_{ej}}{M_\odot} \right)^{-1/2} \ \text{km/s}, \qquad (8)$$

The above estimate shows that one has to observe SNRs in the free expansion stage or closely thereafter, when $V_s \simeq V_{ST}$, in order for the X-ray emission to consist of a nonthermal component.

3 Simulation Method

3.1 Hydrodynamics

We have performed hydrodynamical simulations using the Versatile Advection Code [1](VAC, Tóth, 1996). The calculations have been performed on a spherically symmetric grid with uniform radial grid spacing. As an initial consition we deposit mass and energy in the first few grid cells, this leads to both a forward shock and a reverse shock. At the end of the simulation, the SNR is in its transion stage from the freely expanding stage to the Sedov-Taylor stage, where the reverse shock is propagating into the interior of the SNR. The hydrodynamical simulation yields the fluid velocity of the SNR as a function of radius.
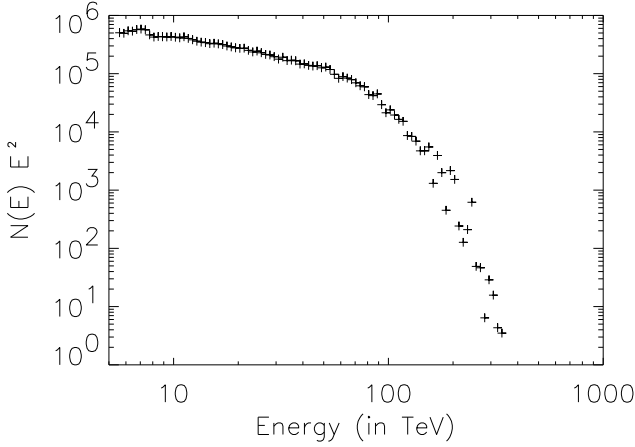
---

[1]See http://www.phys.uu.nl/ toth

Fig. 1. Energy distribution of the total amount of test particles in the SNR.

3.2 Particle acceleration

The acceleration and propagation of particles in a flow can be investigated by solving a Fokker-Planck equation for the particle distribution in phase space (see e.g. Skilling, 1975). Instead we use the stochastic differential equations (SDEs) of the Itô form:

$$\mathrm{d}\boldsymbol{Z} = \dot{\boldsymbol{Z}}\,\mathrm{d}t + \sqrt{2\mathbf{D}} \cdot \mathrm{d}\boldsymbol{W}\ . \tag{9}$$

here $\boldsymbol{Z} = (\boldsymbol{x}\,,\,\boldsymbol{p})$ is the phase-space position vector, $\dot{\boldsymbol{Z}}$ is the phase-space advection velocity and $\mathbf{D}$ is a diffusion tensor, formally defined in dyadic notation as

$$\mathbf{D} \equiv \frac{\langle \Delta \boldsymbol{Z}\,\Delta \boldsymbol{Z} \rangle}{2\Delta t}\ . \tag{10}$$

The noise term $\mathrm{d}\boldsymbol{W}$ in the stochastic term of equation (9) is a N-dimensional Wiener process, where N is the number of degree s of freedom in phase space (e.g MacKinnon & Craig 1991; Achterberg & Krülls 1992 and Krülls & Achterberg 1994). Its components $\mathrm{d}W_i$ satisfy a set of simple rules,

$$\langle \mathrm{d}W_i \rangle = 0 \quad,\quad \langle \mathrm{d}W_i\,\mathrm{d}W_j \rangle = \begin{cases} \mathrm{d}t & \text{if } i = j \\[2mm] 0 & \text{if } i \neq j \end{cases}\ , \tag{11}$$

where the angular brackets indicate an average over many statistically independent realizations of this Wiener process.

By running many independent realizations of prescription (9) one can construct the phase-space distribution $F(\boldsymbol{Z}\,,\,t)$ which corresponds with a solution of a Fokker-Planck equation.

The method allows for a quick simulation method for a given flow, plus one can include effects like synchrotron losses, Inverse Compton losses and Expansion losses.

The application to shock acceleration has already been considered by several authors (e.g. Krülls & Achterberg, 1994; Marcowith & Kirk, 1999), where the results have succesfully been compared with analytical solutions. We employ
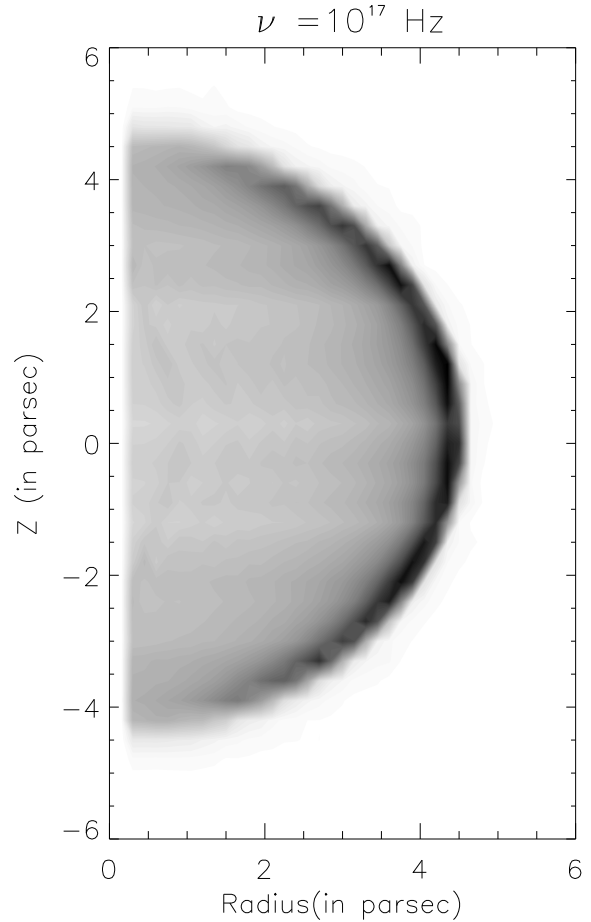

Fig. 2. Synchrotron map at a frequency $\nu = 10^{17}$ Hz

the method in conjunction with the hydrodynamical simulations, in order to calculate the behaviour of the acceleration and propagation of electrons in a young supernova remnant.

3.3 Results

We have simulated the evolution of a single supernova remnant with an energy $E_0 = 10^{51}$ erg, an ejected mass, $M_{\mathrm{ej}} = 6M_{\odot}$ and a constant ISM density of $\rho_0 = 10^{-24}$ g/cm^3. By using the flow of this hydrodynamics simulation, we simultaneously describe the particle acceleration using the SDE method.

We contineously inject particles at the forward shock of the SNR, starting at the age of $t = 200$ years, till the end of the simulation at $t = 1000$ years. All the particles have been injected at a constant injection momentum, p_0, with an injection rate:

$$\mathrm{d}\mathcal{N}(p) \propto R_{\mathrm{snr}}^2\,V_{\mathrm{s}}\,\mathrm{d}t \times \delta(p - p_0)\ , \tag{12}$$

here $\mathrm{d}t$ is the timestep used in the SDE method. Most particles will be injected at late times in the evolution of the SNR. At the end of the simulation, the SNR has a radius of ~ 4.5

parsec. A total of $\sim 4.2 \times 10^6$ test particles are injected throughout the simulation.

The energy distribution of the test particles is shown in figure 1. One can see that the cut-off occurs at $E \simeq 100$ TeV. This is as expected from the theoretical considerations in the above section.

Throughout the simulation we keep track of the magnetic field strength in the supernova remnant by an approach similar to the one used by Duin & Strom (1975). We take an initial uniform magnetic field strength B_0 aligned with the axis of symmetry in the simulation:

$$B_{0r} = B_0 \sin\theta_0 \quad , \quad B_{0\theta} = -B_0 \cos\theta_0 . \tag{13}$$

Throughout the simulation, we can calculate the radial and tangential components B_r and B_θ by using the equations:

$$B_r = \left(\frac{r_0}{r}\right)^2 B_{0r} \quad , \quad B_\theta = \left(\frac{\rho}{\rho_0}\right)\left(\frac{r}{r_0}\right) B_{0\theta} . \tag{14}$$

Here r is the current radial position of the fluid element, and r_0 its position when it crosses the SNR blastwave. Similarly, ρ is the density at the current position of the fluid element and ρ_0 is the density of the ISM. We assume that the only magnetic field present in the SNR is the compressed interstellar field. Because the magnetic field is known throughout the remnant, one can produce synchrotron maps at different frequencies. This can be achieved by calculating for each particle its synchrotron emission profile, by using the tabulated form of $F(\nu/\nu_s)$ (e.g. Rybicky & Lightmann, 1979):

$$P(\nu) = \frac{\sqrt{3}e^3 B \sin\alpha}{m_e c^2} F\left(\frac{\nu}{\nu_s}\right) ; \nu_s \sim \frac{eB}{\pi m_e c}\left(\frac{E}{m_e c^2}\right)^2 \tag{15}$$

An example of such a synchrotron map is shown in figure 2. Furthermore a photon spectrum can be obtained of the whole remnant, by using the same equations from synchrotron theory. The resulting spectrum is depicted in figure 3, where the x-axis is in keV. At the roll-off part of the spectrum we get a spectral index of $\alpha = 3.0$ corresponding with a slope $q = 7.0$. This is encouraging close to the values as observed for five remnants by Allen et al. (1999).

4 Conclusion

We have considered the acceleration of electrons in a young SNR. To that end, we combined a hydrodynamics code with an algorithm to simultaneously calculate the associated acceleration and propagation of electrons. These calculations together with theoretical estimates show that a typical cut-off in the energy spectrum occurs at $E \simeq 100$ Tev, close to the energy of the knee in the cosmic ray spectrum. This confirms shock acceleration as a viable mechanism for cosmic ray production up to the knee, and as the source of the electrons responsible for the nonthermal X-ray emission.

Our method gives similar results as the earlier semi analytical work on this subject by Reynolds (1998), where a
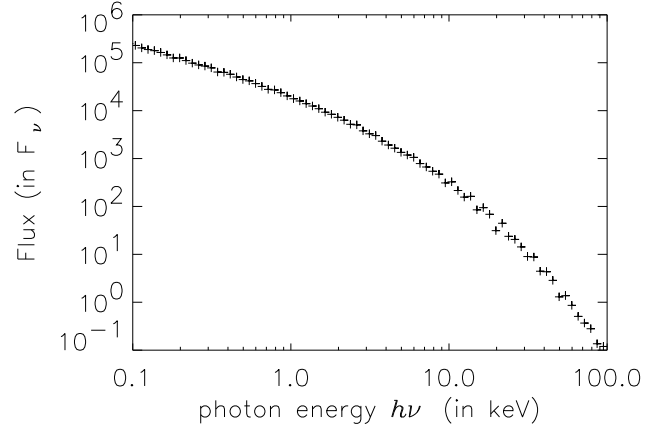

Fig. 3. Total integrated spectrum of the SNR

Sedov-Taylor SNR is assumed throughout the whole evolution of the SNR. We expand on his work by using a hydrodynamics code, which describes the free expansion stage and the transition to the Sedov-Taylor stage.

By using a 2D hydrodynamics code, this method can easily be extended to more complicated configurations, i.e. a non-uniform ISM. In this way one can model SNRs when part of the SNR shell is running into a molecular cloud.

References

Achterberg, A., & Krülls, W.M., A&A, 265, L13, 1992

Allen, G.E., Gotthellf,E.V., Petre, R. 1999, "Evidence of 10-100 Tev Electrons in Supernova Remnants," in Proc. of the 26th ICRC, Salt Lake City, 17-25 August 1999, Edited by D.Kieda,M.Salamon, and B.Dingus, Vol.3, 480-483

Duin, R.M.,& Strom, R.G. , A&A, 39, 33, 1975

Koyama, K., Petre, R., Gotthelf, E.V., Hwang, U., Matsura, M., Ozaki, M.,& Holt,S.S., Nature, 378, 255, 1995

Koyama, K. et al., PASJ, 49, L7, 1997

Krülls, W.M.,Achterberg, A., A&A, 286, 314, 1994

MacKinnon, A. L., Craig, I. J. D., A&A, 251, 693, 1991

Malkov, M.A. and Drury, L.O.'C., Rep. Prog. Phys., 64, 1, 2001.

Marcowith, A., Kirk, J. G., A&A, 256, 157, 1999,

McKee, C.F.,& Truelove, J.K., Phys.Rep., 256, 157, 1995

Reynolds, S.P., ApJ, 493, 375, 1998

Rybicki, G.B., Lightman, A.P. 1979, *Radiative Processes in Astrophysics*, John Wiley & Sons, New York, Ch. 6

Slane, P., Hughes, John P., Edgar, Richard J., Plucinsky, Paul P., Miyata, E., Tsunemi, H., Aschenbach, B., ApJ, 548, 81, 2001

Skilling, J., MNRAS, 172, 557, 1975

Tóth, G., Astrophys. Lett. & Comm., 34, 245, 1996

Woltjer, L., ARA&A, 10, 129, 1972